Inorganic Chemistry

Article

pubs.acs.org/IC

Natural Gas Purification Using a Porous Coordination Polymer with Water and Chemical Stability

Jingui Duan,*[,†] Wanqin Jin,[†] and Rajamani Krishna[‡]

[†]State Key Laboratory of Materials-Oriented Chemical Engineering, College of Chemistry and Chemical engineering, Nanjing Tech University, Nanjing 210009, China

[‡]Van 't Hoff Institute for Molecular Sciences, University of Amsterdam, Science Park 904, 1098 XH Amsterdam, The Netherlands

Supporting Information

ABSTRACT: Porous coordination polymers (PCPs), constructed by bridging the metals or clusters and organic linkers, can provide a functional pore environment for gas storage and separation. But the rational design for identifying PCPs with high efficiency and low energy cost remains a challenge. Here, we demonstrate a new PCP, $[(Cu_4Cl)(BTBA)_8 \cdot (CH_3)_2NH_2) \cdot (H_2O)_{12}] \cdot x$Guest (PCP-33⊃guest), which shows high potential for purification of natural gas, separation of C_2H_2/CO_2 mixtures, and selective removal of C_2H_2 from C_2H_2/C_2H_4 mixtures at ambient temperature. The lower binding energy of the framework toward these light hydrocarbons indicates the reduced net costs for material regeneration, and meanwhile, the good water and chemical stability of it, in particular at pH = 2 and 60 °C, shows high potential usage under some harsh conditions. In addition, the adsorption process and effective site for separation was unravelled by *in situ* infrared spectroscopy studies.

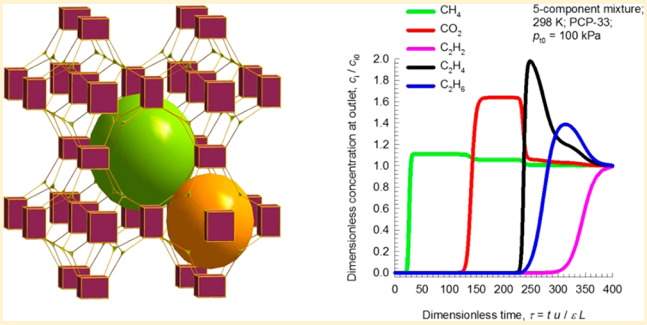

INTRODUCTION

Due to the energy crisis and environmental concerns, the efficient storage and separation of C1 and C2 hydrocarbons (CH_4, C_2H_2, C_2H_4, and C_2H_6) have attracted a great deal of research interest. This is because CH_4 with high heat of combustion (55.7 kJ/g) is poised to become one of the most important energy sources in the future.[1] Acetylene and ethylene are widely used as feedstocks in industrial reactions of polymerization, oxidation, alkylation, hydration, oligomerization, and hydroformylation.[2,3] To produce ethylene, acetylene as the byproduct from the steam cracking of ethane shows deleterious effect to the polyethylene reaction, and also it is well-known to be a highly reactive molecule: it cannot be compressed above 0.2 MPa or it explodes without oxygen, even at room temperature. Furthermore, the separation of C_2H_2/CO_2 mixtures is important in industry for production of pure C_2H_2, which is required for a variety of applications in the petrochemical and electronic industries. The C_2H_2/CO_2 separation is particularly challenging in view of the similarity of the molecular dimensions and boiling points.[4] Thus, the challenges we now face are becoming more practical in nature, that is, how to design and synthesize the safe and effective materials for economic separation.[5−7]

In order to fully utilize these light hydrocarbons, the separations are generally done by cryogenic distillation, which entails high danger and large energy costs. Recently, in contrast with carbon tube[8] and zeolites,[9] a new class of porous materials, porous coordination polymers (PCPs) also called metal−organic frameworks (MOFs),[4,10−21] demonstrate significant promise for such task, since their easy tailorability could lead to higher surface and functional pore environments for different recognition abilities of each component.[22−26] Thus, with great versatility of their structures and pore surface nature, PCP materials have been considered as the most promising candidates for such separations.

Generally, the optimal candidate of PCP materials for gas separation should satisfy at least four important factors:[27−30] (1) high separation selectivity; (2) high separation capacity; (3) good water and chemical stability; (4) low binding energy. Although recent studies showed that some of the strategies, such as immobilizing the strong recognition sites for higher gas selectivity,[31−33] improving the pore volume for higher gas capacity,[34] and enhancing the coordination strength for stable framework,[28,35−37] worked very well in each aspect, the disadvantages of these strategies are also very obvious. For example, the net energy cost for the regeneration process will be increased in frameworks with high binding energies (50−90 kJ/mol), but much lower binding energy will result in lower selectivity.[33] In many cases, the modified frameworks are very sensitive to water and offer significantly reduced pore volume. There is a need to optimize the required characteristics and integrate all of these into one PCP framework. Our objective is the construction of porous coordination polymers for a variety

Received: December 16, 2014
Published: April 17, 2015

DOI: 10.1021/ic5030058
Inorg. Chem. 2015, 54, 4279−4284

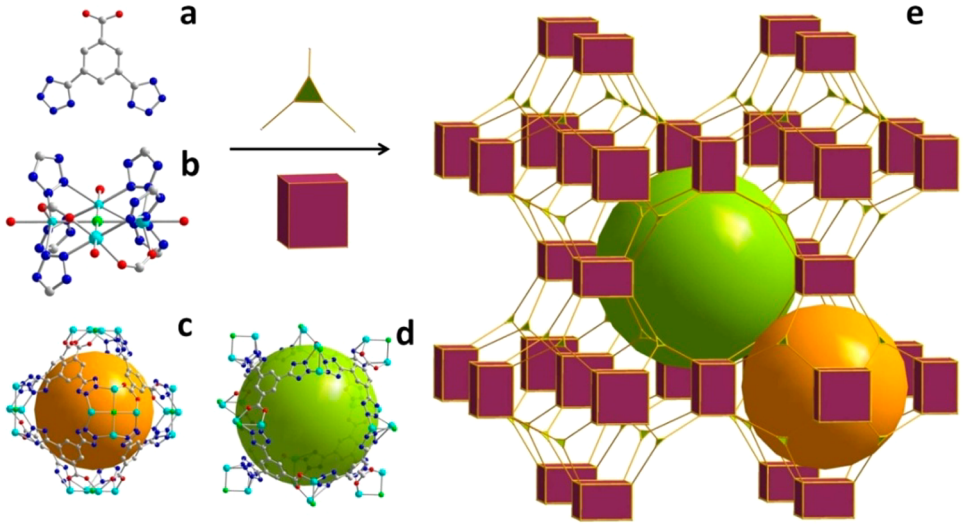

Figure 1. Structure of PCP-33: (a) molecular structure of well designed C_{2v} symmetric ligand (H_3BTBA); (b) the square-planar Cu_4Cl cluster surrounded by six tetrazolate and two carboxylate groups; (c, d) the view of two kinds of cages in PCP-33; (e) the packing view of the 3,8-connected three-dimensional framework derived from the structure of PCP-33.

of applications.[27−29,38] Recently, we reported two water and chemical stable frameworks for selective capture of CO_2. The high coordination number of the La^{3+} atom and well-packed organic walls provide the increased bond energy and hydrophobic environment for a water-resistant framework. However, the heats of adsorption are too low to achieve higher performance for gas separation. In order to further optimize the function of the candidate material, herein, we demonstrate a PCP based on a new C_{2v} symmetric ligand (3,5-bis(2*H*-tetrazol-5-yl)-benzoic acid, H_3BTBA) with heterocoordination groups (Figure 1a). The generated PCP, with suitable pore size distributions and exposed open metal sites, exhibits promising characteristics of high separation capacity and high selectivity of light hydrocarbons at room temperature. In addition, the lower binding energy of the framework toward these light hydrocarbons indicates the reduced net costs for material regeneration, and meanwhile, the good water and chemical stability of it shows high potential for usage under some harsh conditions. Furthermore, the adsorption process and adsorption site for separation was well revealed by using an *in situ* infrared spectroscopy study. Thus, PCP-33 is one of the promising candidates that possess good performance characteristics natural gas purification.

EXPERIMENTAL SECTION

General procedures for the experiments, ligand synthesis, and simulations can be found in the Supporting Information.

Synthesis and Structure of PCP-33. For synthesis of $[(Cu_4Cl)(BTBA)_8\cdot(CH_3)_2NH_2)\cdot(H_2O)_{12}]\cdot x$Guest, (PCP-33·*x*Guest), copper(II) chloride (10 mg), H_3BTBA (6 mg), and HCl (30 μL) were mixed with 2 mL of DMF/H_2O (5:1) in a 4 mL glass container, and the container was tightly capped with a Teflon vial, and the mixture was heated at 65 °C for 2 days. After cooling to room temperature, the resulting green polyhedral crystals were harvested with high yield (65% based on ligand) and washed by DMF.

Solvothermal reaction of $CuCl_2\cdot 2H_2O$ with H_3BTBA in DMF/H_2O containing HCl afforded blue crystals of PCP-33·*x*Guest. Single crystal X-ray diffraction shows that the chloride-centered square-planar $[Cu_4Cl]$ units are linked by eight ligands to form a three-dimensional framework as shown in Figure 1. The cubic sodalite-type framework of PCP-33 is similar as that of Mn-BTT, even though their ligands have different symmetry.[39] The size of the open pore is around 11 Å, while the size of the cross point of the 3-D channel reached 20 Å. In addition, the anionic charge of the framework was balanced by $((CH_3)_2NH_2)^+$, derived from the hydrolysis of DMF in the presence of HCl, which shows a little difference from the counterions ($[Mn(CH_3OH)_6]^{2+}$) in Mn-BTT. The total accessible volume of the fully desolvated PCP-33 is ca. 47.4%, calculated using the PLATON program.[40] The powder X-ray diffraction (PXRD) of the as-synthesized and degassed form of PCP-33 was collected (Figure S6, Supporting Information). With very good reliability factors (R_p = 0.03306 and R_{wp} = 0.04469), Le Bail analysis of as-synthesized form shows that the refined parameters (a = 17.5229 Å) are very close to the data from the single crystal (a = 17.5355(12) Å), reflecting good phase purity and also well-defined structure (Figure S7, Supporting Information). In addition, the peak positions of the degassed form are consistent with its as-synthesized form. Therefore, the framework of PCP-33 is stable even after removing the guest molecules. Thermogravimetric analysis (TG) of PCP-33 shows that PCP-33 is thermally stable up to 200 °C under N_2 atmosphere.

Gas Adsorption. The permanent porosity of desolvated PCP-33 was established by N_2 sorption experiments at 77 K, which exhibits a complete reversible type-I isotherm (Figure 2). The estimated apparent Brunauer−Emmett−Teller surface area is ~1248 $m^2\cdot g^{-1}$ (Langmuir surface ~1419.3 $m^2\cdot g^{-1}$). The calculated pore size distributions according to N_2 isotherm (NLDFT/GCMC method) are in the range 9−22 Å, which matches well the parameters of the

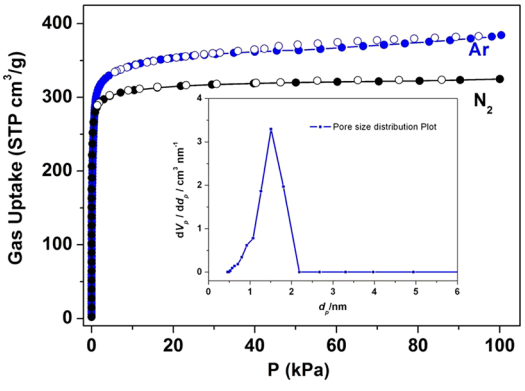

Figure 2. N_2 and Ar adsorption isotherms of PCP-33 at 77 and 87 K. Inset, calculated pore size distributions. The calculated pore volume reached 0.50 $cm^3\cdot g^{-1}$.

DOI: 10.1021/ic5030058
Inorg. Chem. 2015, 54, 4279−4284

crystal structure. The total pore volume calculated from the maximum amount of N_2 adsorbed is 0.50 $cm^3 \cdot g^{-1}$. The C1 and C2 hydrocarbons and CO_2 adsorption isotherms of PCP-33 at 273 and 298 K have been collected and fitted (Figure 3). The Langmuir–Freundlich parameters

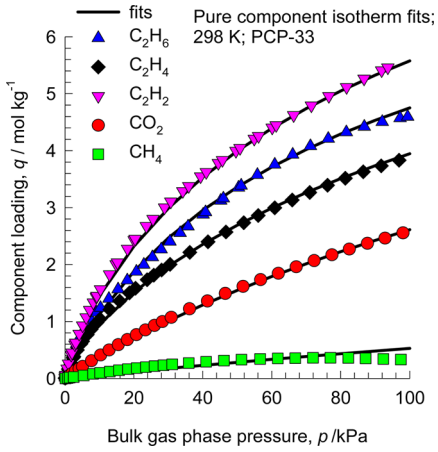

Figure 3. Comparison of absolute component loadings for CH_4, C2 hydrocarbons, and CO_2 at 298 K in PCP-33 with the isotherm fits.

for each pure component isotherms in PCP-33 are provided in Table S1, Supporting Information. The adsorption hierarchies of these five gases are very distinct, indicating good separability. The total uptake of C_2H_2, C_2H_6, C_2H_4, CO_2, and CH_4 in PCP-33 reached 121.8, 102.4, 86.8, 58.6, and 6.9 $cm^3 \cdot g^{-1}$, respectively, at 1 bar and 298 K. In addition, all of the isotherms are completely reversible, and no hysteresis is observed. Thus, these results motivated us to examine the potential application of PCP-33 for C1 and C2 hydrocarbon and CO_2 separation, given the fact that these five molecules have comparable molecular sizes (Table S2, Supporting Information).

Adsorption Selectivity. The ideal adsorbed solution theory (IAST) of Myers and Prausnitz[41] was employed to predict multicomponent adsorption behaviors from the experimental pure-gas isotherms. Figure 4 presents IAST calculations of the component

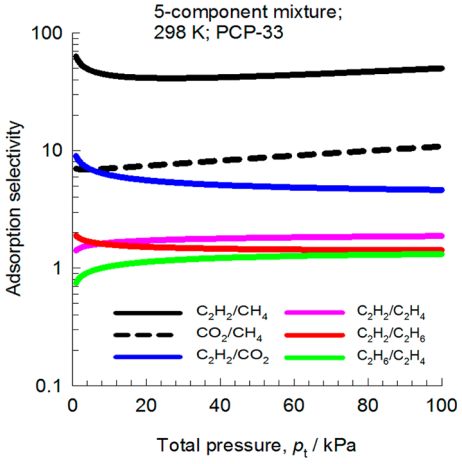

Figure 4. IAST calculations of CH_4, C_2H_2, C_2H_4, C_2H_6, and CO_2 adsorption selectivities in PCP-33 at 298 K.

loadings for CH_4, C_2H_2, C_2H_4, C_2H_6, and CO_2 for adsorption of a five-component equimolar mixture in PCP-33 at 298 K. The IAST calculations show the following loading hierarchies at 100 kPa. On the basis of the component loadings, we calculate the selectivities of separation of the six constituent binary pairs: C_2H_2/CH_4, C_2H_2/C_2H_4, C_2H_2/C_2H_6, C_2H_2/CO_2, C_2H_6/C_2H_4, and CO_2/CH_4. The C_2H_2/CH_4 selectivity is the highest and falls in the range of 40–65, indicating the potential for separation. The predicted CO_2/CH_4 selectivity, as well as the C_2H_2/CO_2 selectivity, is around 6–10. In addition, we note that the equimolar C_2H_2/C_2H_4, C_2H_2/C_2H_6, and C_2H_6/C_2H_4 selectivities are all close to unity, showing the separation of individual components of C2 hydrocarbons is difficult. Thus, the IAST calculations in Figure 4 demonstrate high potential for natural gas purification, as well as the possibility for selective removal of CO_2 from C2 hydrocarbons and separation of C_2H_2/CO_2 mixtures at room temperature.

Isosteric Heat of Adsorption. To understand such high separation ability better, the adsorption enthalpies were calculated. The binding energies of C_2H_2, C_2H_4, C_2H_6, and CO_2 in PCP-33 are reflected in the isosteric heat of adsorption, Q_{st}. These values were determined using the pure component isotherm fits. Figure 5 presents

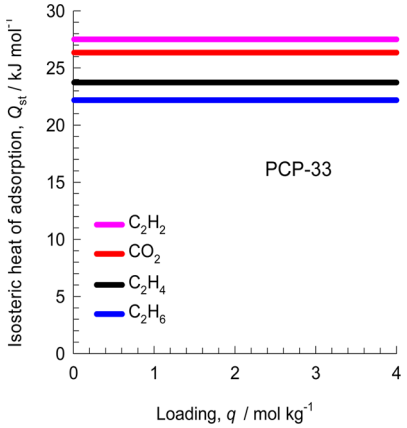

Figure 5. Isosteric heats of adsorption for C_2H_2, C_2H_4, C_2H_6, and CO_2 in PCP-33. The determination of the Q_{st} is based on the Clausius–Clapeyron equation.

data on the loading dependence of Q_{st} for C_2H_2, C_2H_4, C_2H_6, and CO_2 in PCP-33. We note that the binding energies are in the narrow range of 22–27 kJ mol^{-1}. It is particularly note worthy that the Q_{st} for C_2H_2 in PCP-33 is about half the value reported for other MOFs with open metal sites such FeMOF-74, MgMOF-74, CoMOF-74, and CuBTC,[42] implying the significantly lower energy consumption during regeneration of adsorbed C2 hydrocarbons in fixed bed absorbers of PCP-33. This is because the large pore size (9–22 Å) and organic counterions of PCP-33 somewhat reduced the heat of adsorption.[43]

Transient Breakthroughs. We also performed transient breakthrough simulations in a fixed bed adsorber to investigate the separation potential of PCP-33. Such simulations reflect the combined influences of adsorption selectivity and uptake capacity. The breakthroughs of an equimolar component mixture including CH_4, C_2H_2, C_2H_4, C_2H_6, and CO_2, using the methodology described in earlier works,[44,45] were explored at 298 K. The relative concentrations of outflowing gas are shown in Figure 6. The simulation results for transient breakthrough are presented in terms of a *dimensionless* time τ, defined by dividing the actual time, t, by the characteristic time ($L\varepsilon/u$). The breakthrough hierarchy is dictated by the adsorption strengths; the weaker the adsorption, the earlier the breakthrough.

Natural gas usually contains CO_2 and C2 hydrocarbons that require removal by selective adsorption. Figure 6a presents simulation results for equimolar five-component $CH_4/C_2H_2/C_2H_4/C_2H_6/CO_2$ mixtures. The partial pressures of these five gases were set as 20 kPa. It is clear that pure CH_4 can be recovered because it is the least strongly adsorbed component and elutes first. In addition, the result shown in Figure 6b demonstrates that after recovery of CH_4, the remaining $C_2H_2/C_2H_4/C_2H_6/CO_2$ mixture can be separated to yield two fractions: CO_2 and C2 hydrocarbons. Thus, we further simulate the separation behavior of C_2H_2/CO_2, since it is particularly challenging in view of their similarity molecular dimensions and also boiling point.[3] In view of the high selectivity for adsorption of C_2H_2, it is possible to recover pure CO_2 during the adsorption phase in a fixed bed adsorber (Figure 6c). In addition, the significant time interval between the

DOI: 10.1021/ic5030058
Inorg. Chem. 2015, 54, 4279–4284

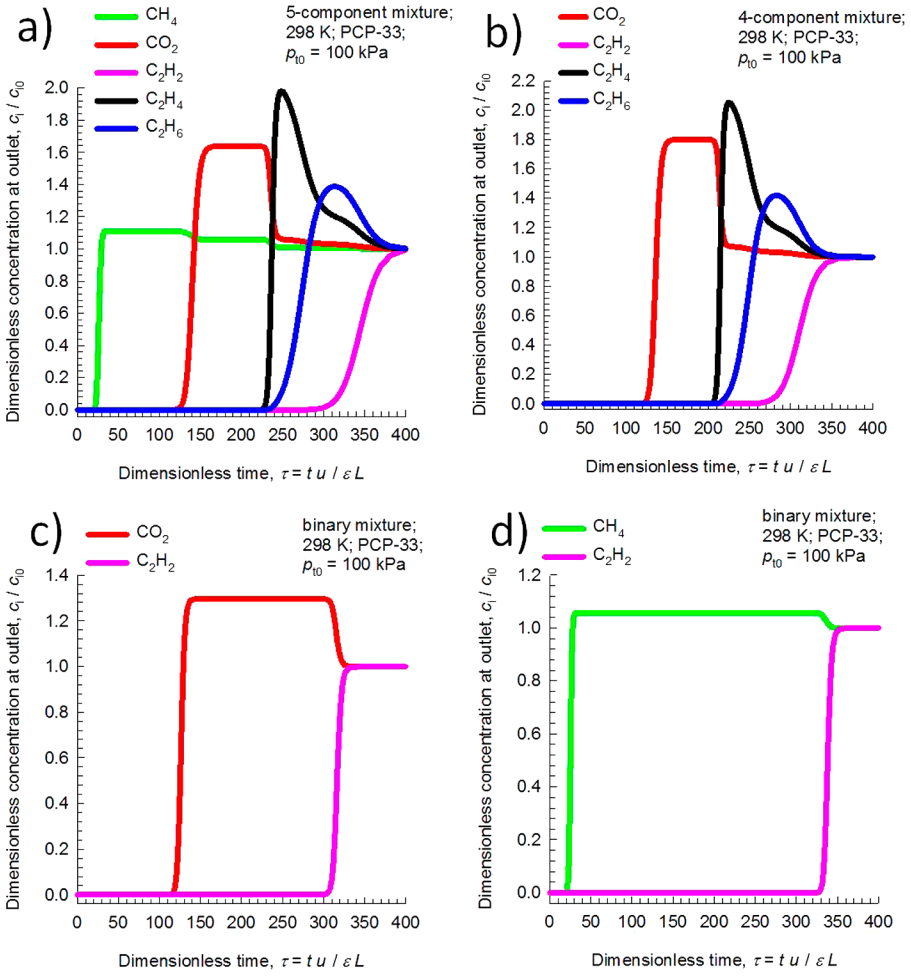

Figure 6. Transient breakthrough simulations for separation of equimolar 5-, 4-, 2-, and 2-component $CH_4/C_2H_2/C_2H_4/C_2H_6/CO_2$ mixtures using PCP-33 at 298 K, with partial pressures of 20, 25, 50, and 50 kPa for each component, respectively.

breakthroughs of C_2H_2 and CH_4 in PCP-33 indicates excellent separation at 298 K (Figure 6d).

We now consider C_2H_2/C_2H_4 separations. In steam cracking of C_2H_6 to produce C_2H_4, one of the byproducts is C_2H_2. C_2H_2 has a deleterious effect on end-products, such as polyethylene. Therefore, recovery or removal of C_2H_2 from C_2H_4 streams is essential. Typically, C_2H_2 forms about 1% of the C_2H_4 streams, and the impurity level of 40 ppm of C_2H_2 needs to be met for C_2H_4 feed to a polymerization reactor. The selective removal of C_2H_2 is conventionally carried out by absorption in dimethylformamide; this process is energy-intensive. Selective adsorption with PCP-33 could be an energy-efficient alternative. The transient breakthrough simulations for C_2H_2/C_2H_4 (1/99) mixtures are shown in Figure 7. We note that for $\tau < 170$, the outlet gas contains less than 40 ppm of C_2H_2. The adsorption cycle needs to be terminated at $\tau = 170$ and the regeneration process needs to be initiated. Due to the significantly low binding energy of C_2H_2 in PCP-33, the regeneration costs can be expected to be lower than that of FeMOF-74, MgMOF-74, CoMOF-74, and CuBTC, which are also suitable for this separation task.[42]

In order to further confirm such high separation capability of PCP-33, pulse chromatographic simulations for varied gas mixtures were carried out. Figure S12, Supporting Information, demonstrates the good potential of PCP-33 for the purification of natural gas. The remaining $C_2H_2/C_2H_4/C_2H_6/CO_2$ mixture can also be separated to yield two fractions: CO_2 and C2 hydrocarbons. In addition, the separation potential of CO_2/C_2H_2 in PCP-33 is clearly indicated. The result of pulse chromatographic simulations match well with that of the breakthrough curves presented in Figure 6.

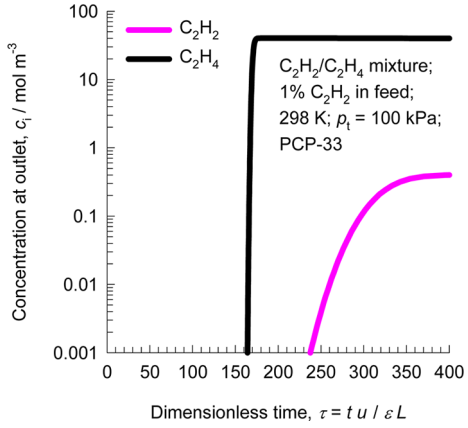

Figure 7. Transient breakthrough of C_2H_2/C_2H_4 mixture containing 1% C_2H_2 mixture in an adsorber bed packed with PCP-33. The partial pressures of C_2H_2 and C_2H_4 in the inlet feed gas mixture are, respectively, p_1 = 1 kPa, p_2 = 99 kPa.

In Situ Infrared Spectroscopy. Although the average adsorption heat of the isolated frameworks can be estimated by the calculation,[46,47] exploring the interactions and adsorption behaviors of the guest on each adsorption site becomes more important, since the precise understanding of the information between host and guest will guide the next material design. Indeed, it is better to load C_2H_2 inside the framework for the IR measurements, but because of its

DOI: 10.1021/ic5030058
Inorg. Chem. 2015, 54, 4279−4284

explosion risk, we employed the typical experiment of PCPs loaded with H_2 for the experiments of in situ infrared spectroscopy.[48]

For the pressure-dependent experiments, the in situ IR was collected following the increased pressure from 0 to 5 bar at 102 K. The collected IR spectra revealed clearly of the procedure of the H_2 adsorption in them (Figure S17a, Supporting Information). For PCP-33, the first peak appears at 4128 cm^{-1} and subsequently grows and shifts to 4130 cm^{-1}, with a weak shoulder at ~4100 cm^{-1}. The bathochromic frequency shifts, from the gas phase value from Raman spectroscopy (4161 cm^{-1}) of the H−H stretching mode of free H_2 molecule, about to 31 cm^{-1}. Thus, the broad nature of the absorption band is attributed to the presence of the binding environments for H_2 at the Cu^{2+} adsorption sites, owing to the partial solvation of the $[Cu_4Cl]^{7+}$ clusters throughout the material and similarly to what was observed in a recent IR study for open metal center PCPs.[48−50] Further, temperature-dependent infrared spectra, shown in Figure S17b, Supporting Information, also confirmed this interaction. One bar of H_2 was dosed into the degassed PCP-33 at 102 K, and the IR spectra were collected at intervals of 10 K increased to final temperature of 172 K. During the temperature ramping, the pressure of the sample cell was maintained at 1 bar. The enthalpy of H_2 adsorbed on this site of PCP-33 was calculated by the peak integrals. The high coverage ΔH_{ads} of these sites is around −4.2 kJ·mol^{-1}, which is lower than that of the adsorption heat of some microframeworks and zeolites.[50,51] This is because, compared with Mn-BTT, the organic counterions of PCP-33 provide weaker interaction toward guest molecules than Mn^{2+} counterions provide.

Water and Chemical Stability of PCP-33. Encouraged by these interesting characters of PCP-33, we determined its water and chemical stability, because such properties of PCP sorbents are the important factors that will possibly restrict their feasible application.[35,52−54] Almost 20000 PCP structures have been reported to date; however, very few of them can maintain their porosity after moisture, water, and chemical treatment,[28,55−57] which is a key challenge for PCP/MOF chemistry. In order to check the stability of PCP-33, fresh crystals were soaked in harsh conditions: hot aqueous HCl (pH = 2), aqueous NaOH (pH = 12), and water solutions for 24 h. After the temperature cooled, we collected the PXRD for each of them. As shown in Figure 8, we found that the PXRD of treated samples are

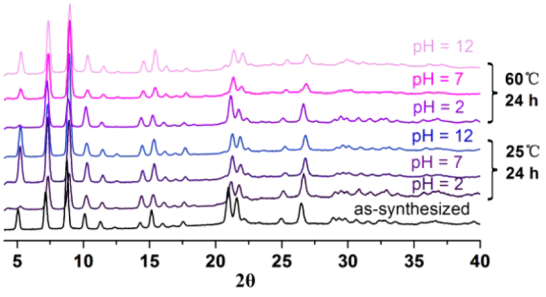

Figure 8. PXRD patterns of water and chemical treated PCP-33.

consistent with their as-synthesized form. Additionally, to further confirm the integrity of the material, CO_2 adsorption isotherms at 195 K for PCP-33 were performed. The gas uptake of treated samples (pH = 2, 7, and 12 at 25 °C; pH = 7 at 60 °C) displaying type I adsorption isotherms are almost same as that of fresh sample. However, the gas uptake of samples that treated under hot aqueous HCl (pH = 2) and aqueous NaOH (pH = 12) decreased very little. Therefore, PCP-33 is a rare sample with good water- and chemical-resistance. Taking the crystal structure and designed ligand into consideration, the high aqueous and chemical stability of PCP-33 should be attributed to the increased coordination bond strength of Cu−N.[35]

CONCLUSIONS

In conclusion, we utilized a heterodonor ligand containing carboxylate and azolate groups and synthesized a new PCP (PCP-33). Adsorption experiments, IAST, breakthrough, and pulse chromatographic simulations strongly demonstrate that it has very high potential to purify natural gas, separate C_2H_2/CO_2 mixtures, and selectively capture of C_2H_2 from C_2H_2/C_2H_4 mixtures at room temperature. More importantly, the good water- and chemical-resistance of this framework indicates realizable separation applications. Thus, we can expected that the promising candidate of PCP-33 will not only offer energy efficient separation of small hydrocarbons in the pressure swing adsorption process but also facilitate the next exploration of PCPs with improved functions.

ASSOCIATED CONTENT

Supporting Information

Synthesis and characterization, PXRD, TGA, IR, sorption isotherms, IAST and breakthrough calculations, isotherm fitting parameters, and video animations of transient breakthrough simulations for five-component mixtures for PCP-33. This material is available free of charge via the Internet at http://pubs.acs.org.

AUTHOR INFORMATION

Corresponding Author

*E-mail: duanjingui@njtech.edu.cn.

Notes

The authors declare no competing financial interest.

ACKNOWLEDGMENTS

The authors gratefully acknowledge the support from Natural Science Foundation of China (No. 21301148).

REFERENCES

(1) Stolaroff, J. K.; Bhattacharyya, S.; Smith, C. A.; Bourcier, W. L.; Cameron-Smith, P. J.; Aines, R. D. *Environ. Sci. Technol.* **2012**, *46*, 6455−6469.
(2) Stang, P. J.; Diederich, F. *Modern Acetylene Chemistry*; VCH: New York, 1995.
(3) Fischer, M.; Hoffmann, F.; Fröba, M. *ChemPhysChem* **2010**, *11*, 2220−2229.
(4) Matsuda, R.; Kitaura, R.; Kitagawa, S.; Kubota, Y.; Belosludov, R. V.; Kobayashi, T. C.; Sakamoto, H.; Chiba, T.; Takata, M.; Kawazoe, Y.; Mita, Y. *Nature* **2005**, *436*, 238−241.
(5) Nugent, P.; Belmabkhout, Y.; Burd, S. D.; Cairns, A. J.; Luebke, R.; Forrest, K.; Pham, T.; Ma, S. Q.; Space, B.; Wojtas, L.; Eddaoudi, M.; Zaworotko, M. J. *Nature* **2013**, *495*, 80−84.
(6) Li, J. R.; Sculley, J.; Zhou, H. C. *Chem. Rev.* **2012**, *112*, 869−932.
(7) Bloch, E. D.; Queen, W. L.; Krishna, R.; Zadrozny, J. M.; Brown, C. M.; Long, J. R. *Science* **2012**, *335*, 1606−1610.
(8) Cinke, M.; Li, J.; Bauschlicher, C. W.; Ricca, A.; Meyyappan, M. *Chem. Phys. Lett.* **2003**, *376*, 761−766.
(9) Choudhary, V. R.; Mayadevi, S. *Sep. Sci. Technol.* **1993**, *28*, 2197−2209.
(10) Furukawa, H.; Ko, N.; Go, Y. B.; Aratani, N.; Choi, S. B.; Choi, E.; Yazaydin, A. O.; Snurr, R. Q.; O'Keeffe, M.; Kim, J.; Yaghi, O. M. *Science* **2010**, *329*, 424−428.
(11) Ma, S. Q.; Sun, D. F.; Simmons, J. M.; Collier, C. D.; Yuan, D. Q.; Zhou, H. C. *J. Am. Chem. Soc.* **2008**, *130*, 1012−1016.
(12) Kitagawa, S.; Kitaura, R.; Noro, S. *Angew. Chem., Int. Ed.* **2004**, *43*, 2334−2375.
(13) Lan, Y. Q.; Jiang, H. L.; Li, S. L.; Xu, Q. *Adv. Mater.* **2011**, *23*, 5015−5020.
(14) Holst, J. R.; Cooper, A. I. *Adv. Mater.* **2010**, *22*, 5212−5216.
(15) Ferey, G.; Mellot-Draznieks, C.; Serre, C.; Millange, F.; Dutour, J.; Surble, S.; Margiolaki, I. *Science* **2005**, *309*, 2040−2042.

DOI: 10.1021/ic5030058
Inorg. Chem. 2015, 54, 4279−4284

(16) Bae, Y. S.; Lee, C. Y.; Kim, K. C.; Farha, O. K.; Nickias, P.; Hupp, J. T.; Nguyen, S. T.; Snurr, R. Q. *Angew. Chem., Int. Ed.* **2012**, *51*, 1857−1860.
(17) Murray, L. J.; Dinca, M.; Long, J. R. *Chem. Soc. Rev.* **2009**, *38*, 1294−1314.
(18) Lee, J. Y.; Pan, L.; Huang, X. Y.; Emge, T. J.; Li, J. *Adv. Funct. Mater.* **2011**, *21*, 993−998.
(19) Vaidhyanathan, R.; Iremonger, S. S.; Shimizu, G. K. H.; Boyd, P. G.; Alavi, S.; Woo, T. K. *Science* **2010**, *330*, 650−653.
(20) Zhang, Y. B.; Zhou, H. L.; Lin, R. B.; Zhang, C.; Lin, J. B.; Zhang, J. P.; Chen, X. M. *Nat. Commun.* **2012**, *3*, No. 642.
(21) Du, M.; Li, C.; Chen, M.; Ge, Z.; Wang, X.; Wang, L.; Liu, C. *J. Am. Chem. Soc.* **2014**, *136*, 10906−10909.
(22) Dinca, M.; Han, W. S.; Liu, Y.; Dailly, A.; Brown, C. M.; Long, J. R. *Angew. Chem., Int. Ed.* **2007**, *46*, 1419−1422.
(23) Ma, S. Q.; Zhou, H. C. *J. Am. Chem. Soc.* **2006**, *128*, 11734−11735.
(24) Van Humbeck, J. F.; McDonald, T. M.; Jing, X. F.; Wiers, B. M.; Zhu, G. S.; Long, J. R. *J. Am. Chem. Soc.* **2014**, *136*, 2432−2440.
(25) He, Y. B.; Zhang, Z. J.; Xiang, S. C.; Fronczek, F. R.; Krishna, R.; Chen, B. L. *Chem.—Eur. J.* **2012**, *18*, 613−619.
(26) Geier, S. J.; Mason, J. A.; Bloch, E. D.; Queen, W. L.; Hudson, M. R.; Brown, C. M.; Long, J. R. *Chem. Sci.* **2013**, *4*, 2054−2061.
(27) Duan, J. G.; Higuchi, M.; Krishna, R.; Kiyonaga, T.; Tsutsumi, Y.; Sato, Y.; Kubota, Y.; Takata, M.; Kitagawa, S. *Chem. Sci.* **2014**, *5*, 660−666.
(28) Duan, J. G.; Higuchi, M.; Horike, S.; Foo, M. L.; Rao, K. P.; Inubushi, Y.; Fukushima, T.; Kitagawa, S. *Adv. Funct. Mater.* **2013**, *23*, 3525−3530.
(29) Duan, J. G.; Yang, Z.; Bai, J. F.; Zheng, B. S.; Li, Y. Z.; Li, S. H. *Chem. Commun.* **2012**, *48*, 3058−3060.
(30) Du, M.; Chen, M.; Yang, X.; Wen, J.; Wang, X.; Fang, S.; Liu, C. *J. Mater. Chem. A* **2014**, *2*, 9828−9834.
(31) Britt, D.; Furukawa, H.; Wang, B.; Glover, T. G.; Yaghi, O. M. *Proc. Natl. Acad. Sci. U.S.A.* **2009**, *106*, 20637−20640.
(32) McDonald, T. M.; D'Alessandro, D. M.; Krishna, R.; Long, J. R. *Chem. Sci.* **2011**, *2*, 2022−2028.
(33) Demessence, A.; D'Alessandro, D. M.; Foo, M. L.; Long, J. R. *J. Am. Chem. Soc.* **2009**, *131*, 8784−8785.
(34) Yuan, D. Q.; Zhao, D.; Sun, D. F.; Zhou, H. C. *Angew. Chem., Int. Ed.* **2010**, *49*, 5357−5361.
(35) Choi, H. J.; Dinca, M.; Dailly, A.; Long, J. R. *Energy Environ. Sci.* **2010**, *3*, 117−123.
(36) Makal, T. A.; Wang, X.; Zhou, H. C. *Cryst. Growth Des* **2013**, *13*, 4760−4768.
(37) Ma, D. Y.; Li, Y. W.; Li, Z. *Chem. Commun.* **2011**, *47*, 7377−7379.
(38) Duan, J. G.; Higuchi, M.; Foo, M. L.; Horike, S.; Rao, K. P.; Kitagawa, S. *Inorg. Chem.* **2013**, *52*, 8244−8249.
(39) Dinca, M.; Dailly, A.; Liu, Y.; Brown, C. M.; Neumann, D. A.; Long, J. R. *J. Am. Chem. Soc.* **2006**, *128*, 16876−16883.
(40) Spek, A. L. *J. Appl. Crystallogr.* **2003**, *36*, 7−13.
(41) Myers, A. L.; Prausnitz, J. M. *AIChE J.* **1965**, *11*, 121−130.
(42) He, Y.; Krishna, R.; Chen, B. *Energy Environ. Sci.* **2012**, *5*, 9107−9120.
(43) Klein, N.; Senkovska, I.; Gedrich, K.; Stoeck, U.; Henschel, A.; Mueller, U.; Kaskel, S. *Angew. Chem., Int. Ed.* **2009**, *48*, 9954−9957.
(44) Krishna, R. *Microporous Mesoporous Mater.* **2014**, *185*, 30−50.
(45) Krishna, R.; Long, J. R. *J. Phys. Chem. C* **2011**, *115*, 12941−12950.
(46) Rowsell, J. L. C.; Yaghi, O. M. *J. Am. Chem. Soc.* **2006**, *128*, 1304−1315.
(47) Sumida, K.; Stuck, D.; Mino, L.; Chai, J. D.; Bloch, E. D.; Zavorotynska, O.; Murray, L. J.; Dinca, M.; Chavan, S.; Bordiga, S.; Head-Gordon, M.; Long, J. R. *J. Am. Chem. Soc.* **2013**, *135*, 1083−1091.
(48) Vitillo, J. G.; Regli, L.; Chavan, S.; Ricchiardi, G.; Spoto, G.; Dietzel, P. D. C.; Bordiga, S.; Zecchina, A. *J. Am. Chem. Soc.* **2008**, *130*, 8386−8396.
(49) Peterson, V. K.; Liu, Y.; Brown, C. M.; Kepert, C. J. *J. Am. Chem. Soc.* **2006**, *128*, 15578−15579.
(50) Arean, C. O.; Chavan, S.; Cabello, C. P.; Garrone, E.; Palomino, G. T. *ChemPhysChem* **2010**, *11*, 3237−3242.
(51) Palomino, G. T.; Bonelli, B.; Arean, C. O.; Parra, J. B.; Carayol, M. R. L.; Armandi, M.; Ania, C. O.; Garrone, E. *Int. J. Hydrogen Energy* **2009**, *34*, 4371−4378.
(52) Colombo, V.; Galli, S.; Choi, H. J.; Han, G. D.; Maspero, A.; Palmisano, G.; Masciocchi, N.; Long, J. R. *Chem. Sci.* **2011**, *2*, 1311−1319.
(53) Park, K. S.; Ni, Z.; Cote, A. P.; Choi, J. Y.; Huang, R. D.; Uribe-Romo, F. J.; Chae, H. K.; O'Keeffe, M.; Yaghi, O. M. *Proc. Natl. Acad. Sci. U.S.A.* **2006**, *103*, 10186−10191.
(54) Taylor, J. M.; Dawson, K. W.; Shimizu, G. K. H. *J. Am. Chem. Soc.* **2013**, *135*, 1193−1196.
(55) Cychosz, K. A.; Matzger, A. J. *Langmuir* **2010**, *26*, 17198−17202.
(56) Kandiah, M.; Nilsen, M. H.; Usseglio, S.; Jakobsen, S.; Olsbye, U.; Tilset, M.; Larabi, C.; Quadrelli, E. A.; Bonino, F.; Lillerud, K. P. *Chem. Mater.* **2010**, *22*, 6632−6640.
(57) Feng, D. W.; Gu, Z. Y.; Li, J. R.; Jiang, H. L.; Wei, Z. W.; Zhou, H. C. *Angew. Chem., Int. Ed.* **2012**, *51*, 10307−10310.

DOI: 10.1021/ic5030058
Inorg. Chem. 2015, 54, 4279−4284

Natural Gas Purification Using a Porous Coordination Polymer with Water and Chemical Stability

Jingui Duan, *[a] Wanqin Jin, [a] and Rajamani Krishna, [b]

[a] State Key Laboratory of Materials-Oriented Chemical Engineering, College of Chemistry and Chemical engineering, Nanjing Tech University, Nanjing, 210009, China. Email: duanjingui@njtech.edu.cn

[b] Van 't Hoff Institute for Molecular Sciences, University of Amsterdam, Science Park 904, 1098 XH Amsterdam, The Netherlands.

General Procedures and Materials.

All air-sensitive reactions were carried out under a dry nitrogen atmosphere using standard Schlenk techniques. All the reagents and solvents were commercially available and used as received. The FTIR spectra were recorded in the range of 4000-400 cm^{-1} on a Nicolet ID5 ATR spectrometer. Thermal analyses were performed on a Rigaku TG8120 instruments from room temperature to 600 °C at a heating rate of 5 °C/min under flowing nitrogen. ^{1}H and ^{13}C NMR spectra were recorded on a Bruker 500 FT-NMR spectrometer. Powder X-ray diffraction (PXRD) patterns were collected using a Bruker AXS D8 Discover powder diffractometer equipped with a Cu Ka X-ray source at 40 kV, 40 mA. Simulated powder patterns from single-crystal X-ray diffraction data were generated using Mercury 1.4.2 software. For in-situ infrared spectroscopy, the samples were evacuated at 333 K for 6 h, and final activation was performed under a high vacuum by heating to 393 K for another 12h. IR were collected using a Thermo Scientific Nicolet 6700 FTIR spectrometer equipped with a cryogenic detector with the sample compartment modified to accommodate the cryogenic head. The final spectra were each recorded at the resolution of 0.125 cm^{-1}.

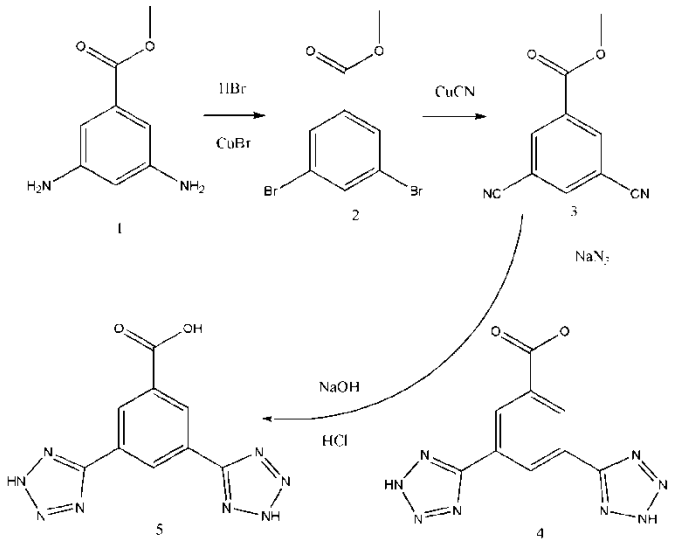

Scheme S1 The route for the ligand synthesis.

Synthesis of organic ligand

Synthesis of 3,5-Dibromo-benzoic acid methyl ester (2)

3,5-Diamino-benzoic acid methyl ester (7.9 g, 47.6 mmol) was dissolved in 220 ml 20% HBr solution, cooled to 0 ℃. 50 ml of 2.5 M sodium nitrite solution was added slowly accompanied by the rapid stirring, giving a solution of diazonium bromide. The

solution of diazonium bromide was added to solution containing 19.8 g CuBr and 90 ml HBr solution (20%) under stirring, and the temperature was kept under 0 ℃. After the addition was completed, it is kept on stirring under room temperature for 5 h. Compound 2 (9.8 g, 33.6 mmol) was obtained. ^{1}H NMR ($CHCl_3$) δ : 8.11 (s，2H) , 7.82 (s, 1H), 3.90 (s, 3H).

Synthesis of 3,5-Dicyano-benzoic acid methyl ester (3)

3,5-Dibromo-benzoic acid methyl ester (1 g, 3.4 mmol) was dissolved in dry NMP (30 ml) and copper cyanide (1.2 g, 13.6 mmol) was added, the reaction mixture was heated to 160℃ under N2 for 24 h. After the temperature cool down, the solution was quenched with saturated NH4Cl solution. The reaction mixture was diluted with EtoAc and filtered through celite plug. The filter was diluted with water and brine. The solvent was evaporated and then the residue was purified by silica gel column chromatography using hexane/CH_2Cl_2 as eluent to give compound 3 as a pure white solid (0.35 g, 18.8 mmol). ^{1}H NMR ($CHCl_3$) δ : 8.07 (s，2H) , 7.79 (s, 1H), 3.896 (s, 3H).

Synthesis of 3,5-Bis-(2H-tetrazol-5-yl)-benzoic acid (5: H_3TBA)

A mixture of 3,5-Dicyano-benzoic acid methyl ester (0.258 g, 1.387 mmol), NaN_3 (0.542 g, 8.32 mmol), and triethylamine hydrochloride (1.14 g, 8.32 mmol) in 15 mL of toluene and 3 mL of methanol was heated at reflux in a 50-mL round-bottom flask for 3 days. Upon cooling to room temperature, 15 mL of an aqueous solution of NaOH (1 M) was added, and the mixture was stirred for 30 min. The aqueous layer was treated with ca. 20 mL of diluted HCl (1 M) until no further white precipitate formed. The precipitate was then collected by filtration, dried in the air, and dissolved in aqueous NaOH (1 M). The resulting clear, colorless solution was titrated with diluted HCl (1 M) until the pH of the solution was 4-5. The ensuing white precipitate was washed with successive aliquots of distilled water, methanol, and acetone to afford white product. ^{1}H NMR (DMSO-*d*6) δ : 8.96 (s, 1H), 8.74 (s, 2H). MS (calc.) m/z = 257.65 $[M-H]^-$.

Caution! Metal azides are water sensitive and potentially explosive and should be handled with care.

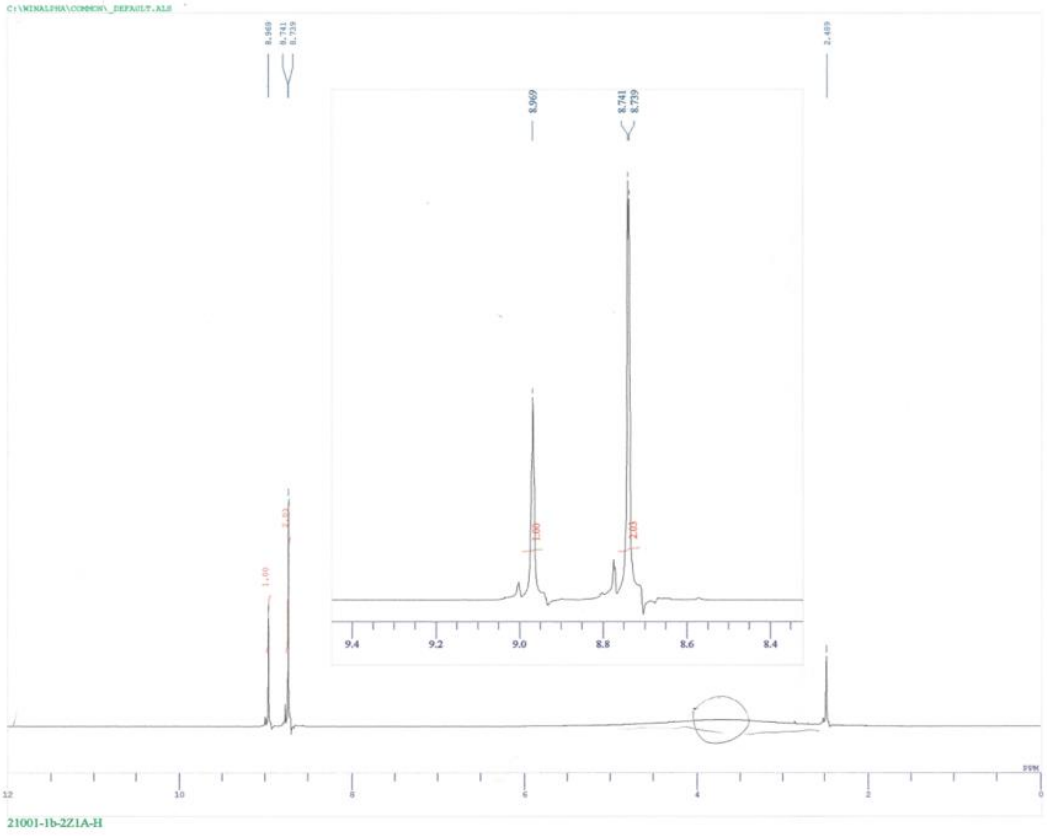

Fig. S1 ^{1}H NMR spectra of H_3L

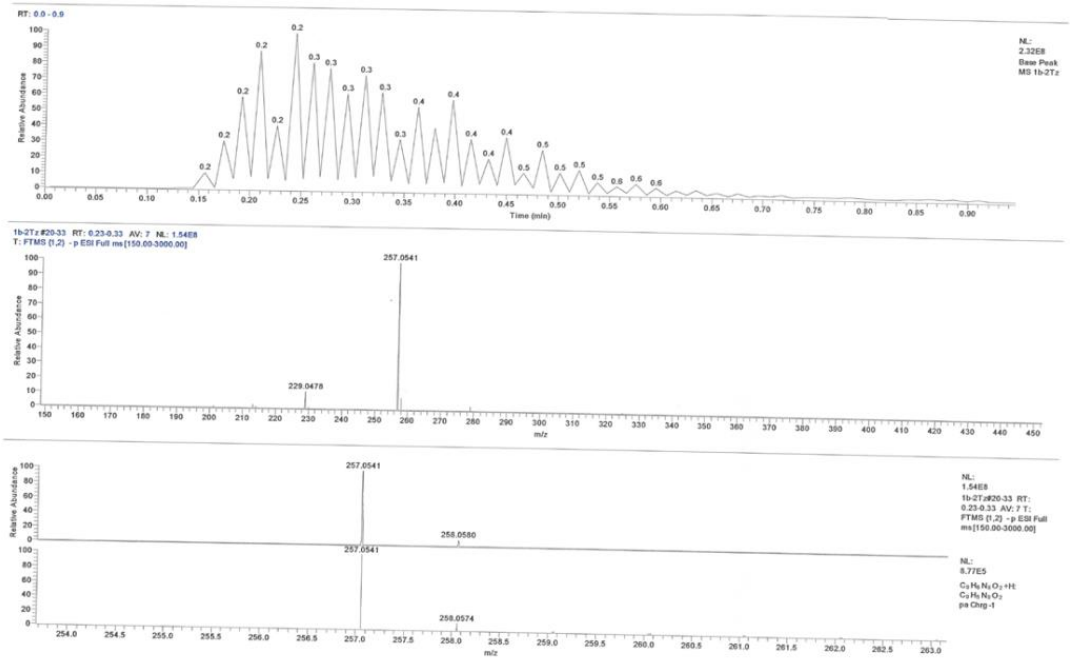

Fig. S2 Mass spectra of H_3L

Synthesis of PCP-33.

Synthesis of $[(Cu_4Cl)_3(TBA^{3-})_8 \cdot (H_2O)_{12}] \cdot xG$ (G = solvent molecules), (PCP-33): copper(II) chloride (10 mg), H_3TBA, 6 mg) and HCl (30 μL) were mixed with 2 ml of DMF/H_2O (5:1) in a 4 mL glass container and tightly capped with a Teflon vial and heated at 65 °C for two days. After cooling to room temperature, the resulting green polyhedral crystals were harvested and washed with DMF.

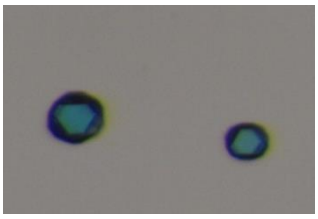

Single crystal X-ray studies.

The single crystal X-ray diffraction measurement was performed at 173 K with a Rigaku AFC10 diffractometer with Rigaku Saturn Kappa CCD system equipped with a MicroMax-007 HF/VariMax rotating-anode X-ray generator with confocal monochromated MoKα radiation. Data were processed using Crystal Clear TM-SM (Version 1.4.0). The structure was solved by direct methods and refined using the full-matrix least squares technique using the SHELXTL package[1]. Nonhydrogen atoms were refined with anisotropic displacement parameters during the final cycles. Organic hydrogen atoms were placed in calculated positions with isotropic displacement parameters set to 1.2Ueq of the attached atom. The unit cell includes a large region of disordered solvent molecules, which could not be modeled as discrete atomic sites. We employed PLATON/SQUEEZE[2,3] to calculate the diffraction contribution of the solvent molecules and, thereby, to produce a set of solvent-free diffraction intensities; the structure was then refined again using the data generated.

Adsorption Experiments.

Before the measurement, the solvent-exchanged sample (about 100 mg) was prepared by immersing the as-synthesized samples in acetone for three days to remove the nonvolatile solvents, and the extract was decanted every 8 h and fresh methanol was replaced. The completely activated sample was obtained by heating the solvent-exchanged sample at 120 °C under a dynamic high vacuum for 20 h. In the gas adsorption measurement, ultra-high-purity grade were used throughout the

adsorption experiments. Gas adsorption isotherms were obtained using a Belsorp-mini volumetric adsorption instrument from BEL Japan Inc. using the volumetric technique. To provide high accuracy and precision in determining P/P_0, the saturation pressure P_0 was measured throughout the N_2 analyses by means of a dedicated saturation pressure transducer, which allowed us to monitor the vapor pressure for each data point.

Water and chemical stability experiments

For chemical treatment, fresh PCP-33 was soaked in DMF for two days (for removing the uncoordinated ligands) and then changed the solvents to methanol for another two days. During these two days, the methanol was changed by fresh methanol in each eight hours. PCP-33 (around 60 mg for each) was soaked into six bottles with water (4 ml), respectively. HCl and NaOH were used to turn the pH of the solution to 2, 7 and 12. Three bottles were kept at 25℃ for 24 h and another three were kept at 60℃ for 24 h. After the temperature cooling down, partial samples were used for PXRD patterns collections and partial samples were used for gas sorption works (washed by methanol three times and degassed at 120°C for 24h.

Fitting of pure component isotherms

The experimentally measured excess loadings for CH_4, C_2H_2, C_2H_4, C_2H_6, and CO_2 in PCP-33 at temperatures of 273 K, and 298 K were first converted to absolute loadings using the procedure described in detail by Wu et al.[4] For the purpose the pore volume of 0.5024 cm^3/g was used.

The isotherm data at both temperatures were fitted with the Langmuir-Freundlich model

$$q = q_{sat}\frac{bp^{\nu}}{1+bp^{\nu}}$$

with *T*-dependent parameter *b*

$$b_A = b_0 \exp\left(\frac{E}{RT}\right)$$

The fitted parameter values are presented in Table s1.

As illustration of the goodness of the fits, Fig 2 and Fig S8 present a comparison of absolute component loadings for CH_4, C_2H_2, C_2H_4, C_2H_6, and CO_2 at 298 K, and 273

K in PCP-33 with the isotherm fits. The fits are good for all components over the entire pressure range.

Isosteric heat of adsorption

are reflected in For use of PCP-33 in a pressure swing adsorption device, the binding energies of C_2H_2, C_2H_4, C_2H_6, and CO_2 in PCP-33 are important, because they largely dictate the energy required in the regeneration cycle. The isosteric heat, Q_{st}, defined as

$$Q_{st} = RT^2\left(\frac{\partial \ln p}{\partial T}\right)_q$$

were determined using the pure component isotherm fits. The calculations of, Q_{st}, are based on the use of the Clausius-Clapeyron equation.

Calculations of adsorption selectivity

The data on the pure component isotherms, along with the isosteric heats of adsorption indicate that it is possible recover pure methane from a mixture containing a wide variety of impurities such as CH_4, C_2H_2, C_2H_4, C_2H_6, and CO_2. The selectivity of preferential adsorption of component 1 over component 2 in a mixture containing 1 and 2, perhaps in the presence of other components too, can be formally defined as

$$S_{ads} = \frac{q_1/q_2}{p_1/p_2}$$

Here, q_1 and q_2 are the *absolute* component loadings of the adsorbed phase in the mixture. In all the calculations to be presented below, the calculations of S_{ads} are based on the use of the Ideal Adsorbed Solution Theory (IAST) of Myers and Prausnitz.[5]

Packed bed absorber breakthrough simulations

Fixed bed, packed with crystals of nanoporous materials, are commonly used for separation of mixtures such adsorbers are commonly operated in a transient mode, and the compositions of the gas phase, and within the crystals, vary with position and time. For a given separation task, transient breakthroughs provide more a realistic evaluation of the efficacy of a material, as they reflect the combined influence of adsorption selectivity, and adsorption capacity.[6,7] To demonstrate the separation

potential of PCP-33, we carried out a series of transient breakthrough simulations using the methodology described in earlier works.[6-8]

For each separation task, two types of simulations were conducted.

(a) Pulse chromatographic simulations with injection of a short duration pulse of the mixture to be separated. For simulation of pulse chromatographic separations, we use the inlet conditions

$$0 \le t \le t_0; \quad p_i(0,t) = p_{i0}; \quad u(0,t) = u$$

where the time for duration of the pulse is t_0, and u is the superficial gas velocity at the inlet to the adsorber. Subsequent to pulse injection, the adsorbed components are desorbed by use of purge inert gas.

(b) Breakthrough simulations in which at time, $t = 0$, the inlet to the adsorber, $z = 0$, is subjected to a step input of the gas mixture and this step input is maintained till the end of the adsorption cycle when steady-state conditions are reached.

$$t \ge 0; \quad p_i(0,t) = p_{i0}; \quad u(0,t) = u$$

The simulation results for transient breakthrough are presented in terms of a *dimensionless* time, τ, defined by dividing the actual time, t, by the characteristic time, $\frac{L\varepsilon}{u}$. For the transient breakthrough simulations presented in this article, the following parameter values were used: framework density of PCP-33. ρ = 1261 kg m^{-3}; length of packed adsorber bed, L = 1 m; fractional voidage of packed bed, ε = 0.4; superficial gas velocity at inlet to the adsorber, u= 0.04 m/s; time duration of pulse, t_0 = 10 s.

Estimation of the isosteric heats by temperature-dependent IR

The equations we used for the calculation of enthalpy and entropy[9]:

Langmuir isotherm:

$$\boldsymbol{q=A/A_M=K(T)p/[1+K(T)p]} \qquad (5)$$

where q is the coverage, A is the intensity of the IR adsorption band and A_M stands for the intensity correspoding to full coverage (q =1). K is adsorption equilibrium constant and p is the equilibrium pressure.

Vant't Hoff equation:

$$\boldsymbol{K(T)=\exp(-\Delta H^0/RT)\exp(\Delta S^0/R)} \qquad (6)$$

the combination of the vant't Hoff and Langmuir equations lead to the VTIR

equation:

$$ln[A/(A_M-A)p]=(-\Delta H^0/RT)+(\Delta S^0/R) \quad (7)$$

Plot the left-hand side of Equation (3) against the reciprocal of the temperature.

In addition, three assumptions, the Lambert-Beer law is valid; the adsorption process is an ideal Langmuir-type process; both ΔH^0 and ΔS^0 are temperature independent, should be taken into the considerations.

Notation

b	Langmuir constant, $Pa^{-\nu_i}$
L	length of packed bed adsorber, m
p_i	partial pressure of species *i* in mixture, Pa
p_t	total system pressure, Pa
q_i	component molar loading of species *i*, mol kg^{-1}
q_t	total molar loading in mixture, mol kg^{-1}
q_{sat}	saturation loading, mol kg^{-1}
R	gas constant, 8.314 J mol^{-1} K^{-1}
t	time, s
T	absolute temperature, K
u	superficial gas velocity in packed bed, m s^{-1}
z	distance along the adsorber, and along membrane layer, m

Greek letters

ε	voidage of packed bed, dimensionless
ρ	framework density, kg m^{-3}
τ	time, dimensionless

Subscripts

i	referring to component *i*
t	referring to total mixture

Structure information

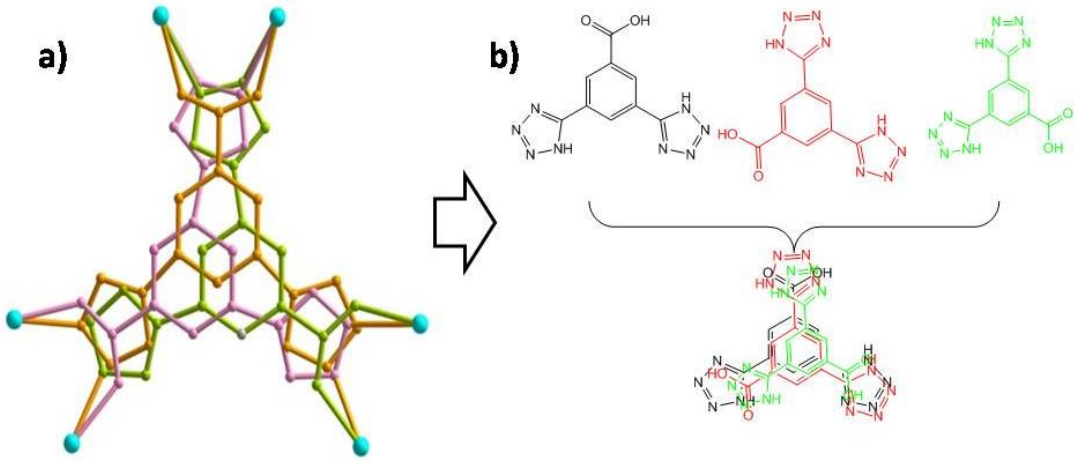

Fig. S3 The disordered ligand in PCP-33. In PCP-33, the symmetry of involved ligand is C_{2v}, however, the generated space group of final structure is $P_{m\text{-}3m}$. Therefore, the connection of one ligand to three clusters will show three possible directions (highlighted by different colors).

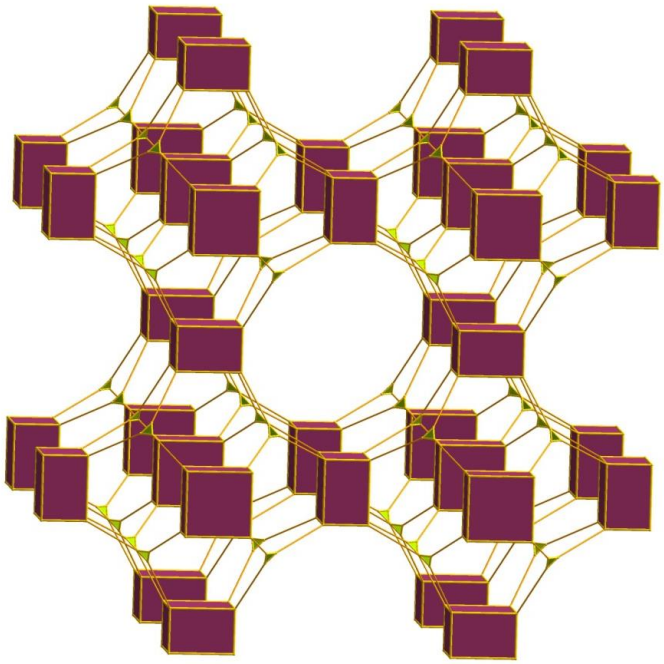

Fig. S4 The SOD topology of PCP-33.

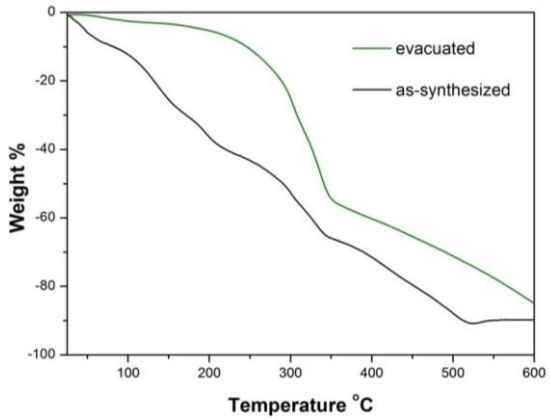

Fig. S5 TG of PCP-33**:** as-synthesized samples (black) and completely activated samples (green).

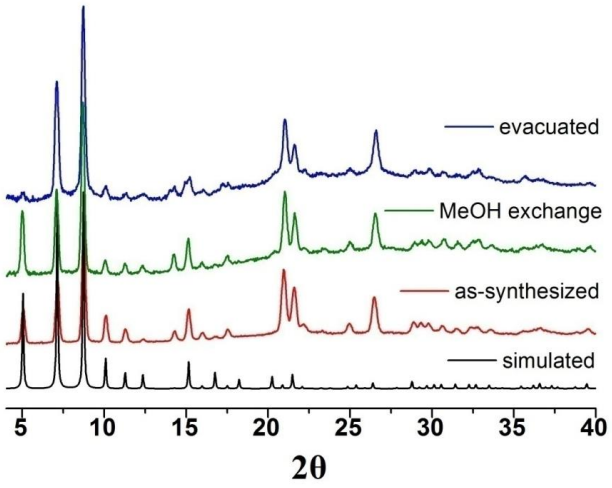

Fig. S6 The PXRD patterns of PCP-33.

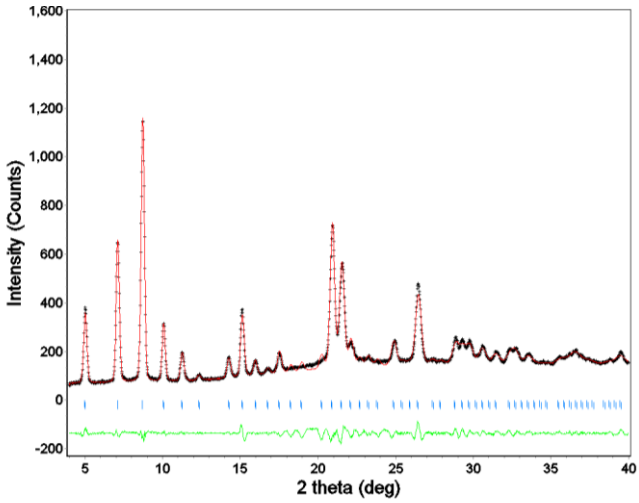

Fig S7 The results of Le Bail analysis for the PXRD of as-synthesized PCP-33. Refined parameters and reliability factors are as follows: space group, $P_{m\text{-}3m}$, a = 17.5229 Å, R_p = 0.03306 and R_{wp} = 0.04469

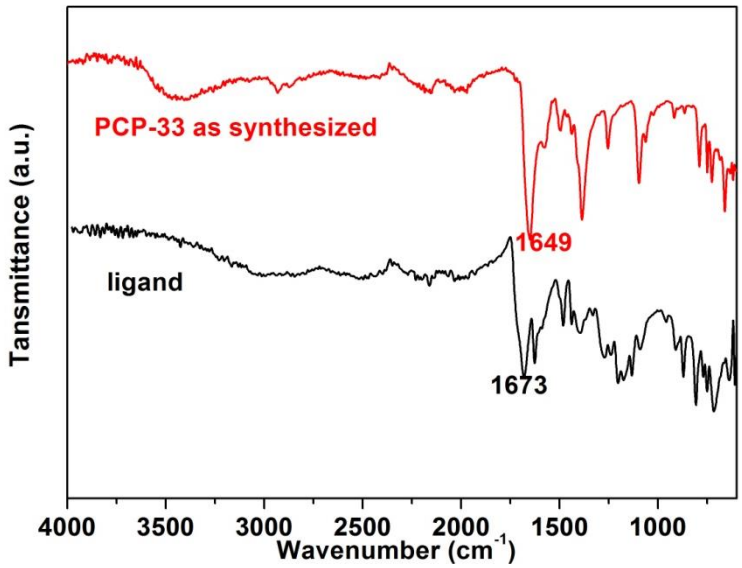

Fig. S8 Infrared spectra of as-synthesized PCP-33 and ligand.

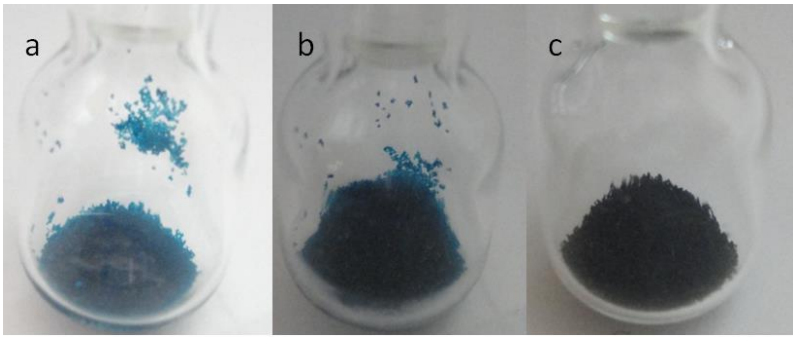

Fig. S9 Visual observation of colour change of PCP-33 upon activation, and (c) completely activated samples.

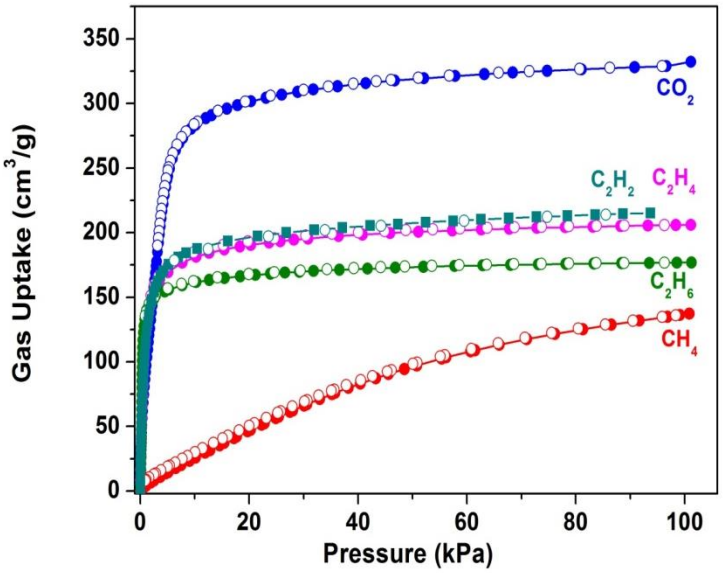

Fig. S10 Low pressure gas adsorption of PCP-33 at 195K.

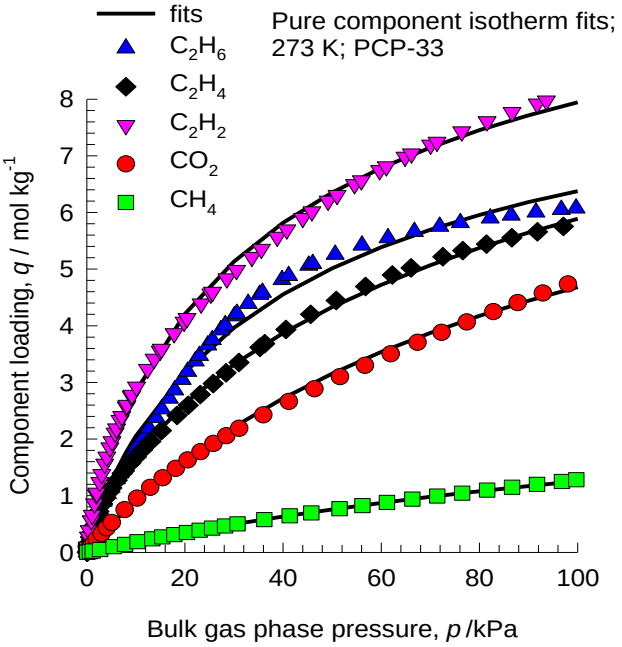

Fig. S11 Comparison of absolute component loadings for CH_4, C_2H_2, C_2H_4, C_2H_6, and CO_2 at 273 K in PCP-33 with the isotherm fits.

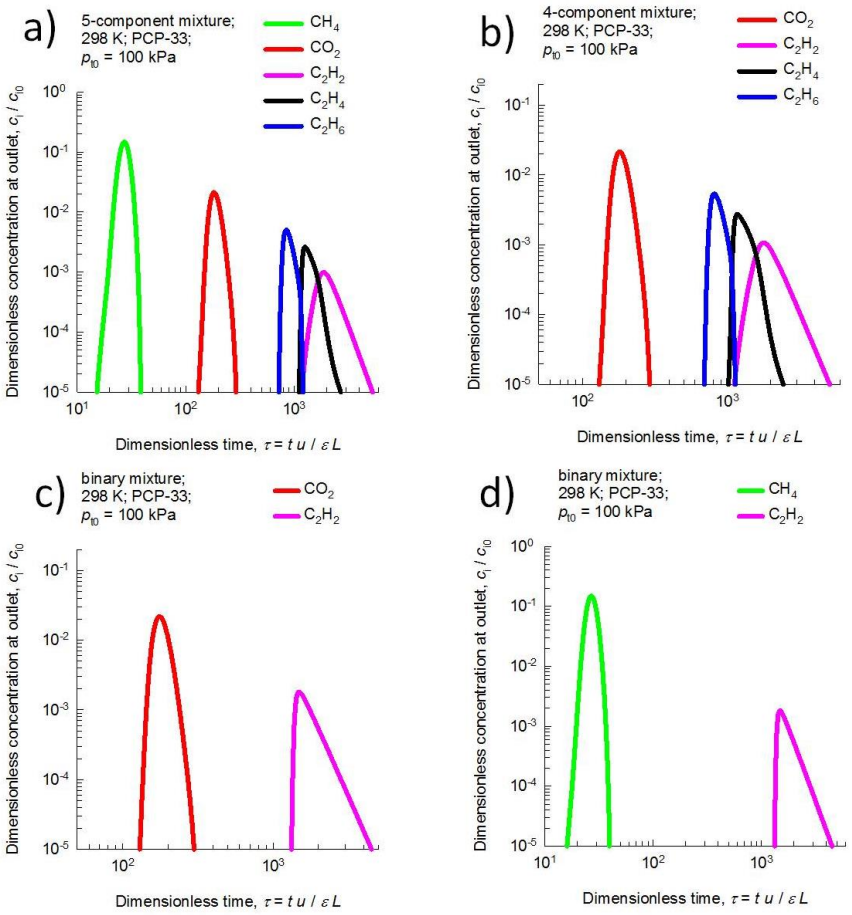

Fig. S12 Pulse chromatographic simulations of the absorber packed in PCP-33 and maintained at isothermal conditions at 298 K.

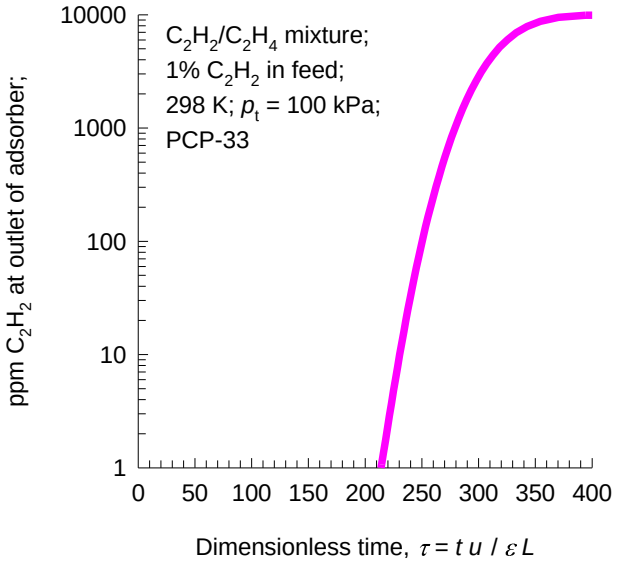

Fig. S13 Ppm C_2H_2 in the gas mixture exiting the adsorber. The total bulk gas phase is at 298 K and 100 kPa. The partial pressures of C_2H_2, and C_2H_4 in the inlet feed gas mixture are, respectively, p_1 = 1 kPa, p_2 = 99 kPa.

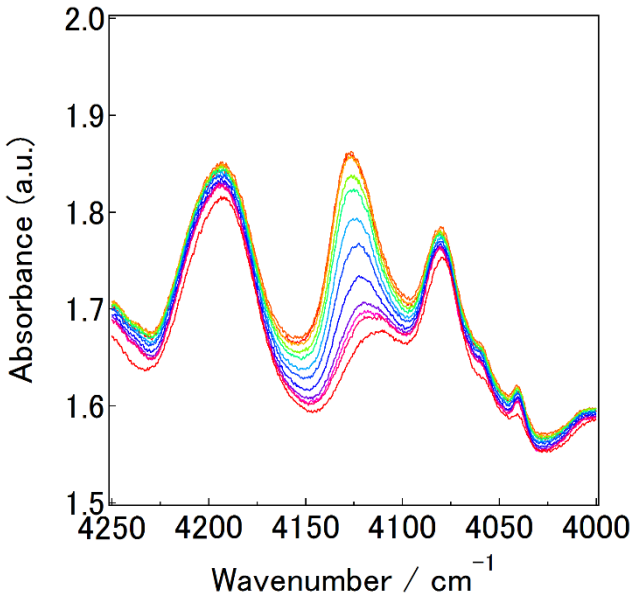

Fig. S14 Original pressure-dependent infrared spectra for H_2 binding within PCP-33 at 102K. The resolution of in-situ IR is 0.125cm^{-1}.

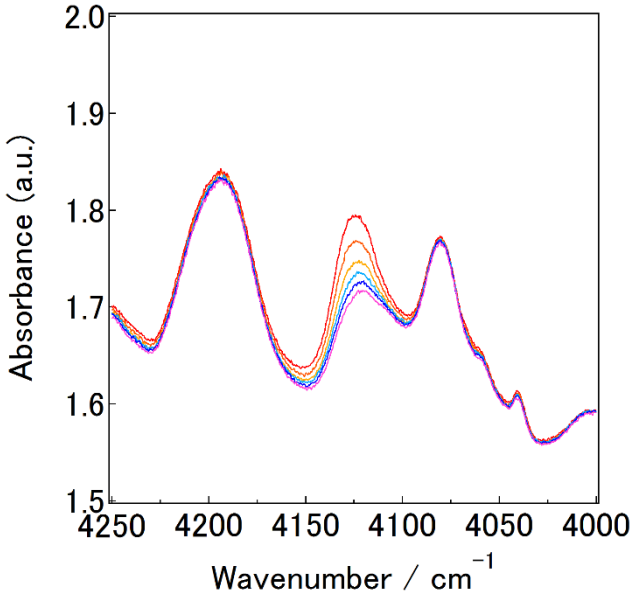

Fig. S15 Original temperature-dependent infrared spectra for H_2 binding within PCP-33 at 1 bar. The resolution of in-situ IR is 0.125cm^{-1}.

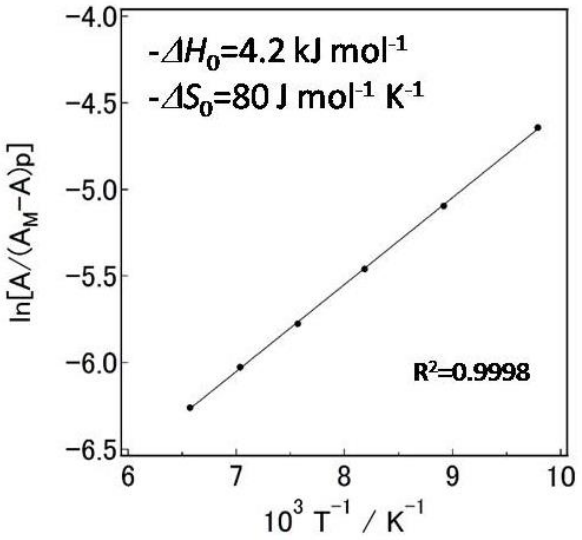

Fig. S16 An Arrhenius-type plot derived from the integral of absorption band corresponding to the binding site for PCP-33. The solid lines represent the line of best fit to each set of data.

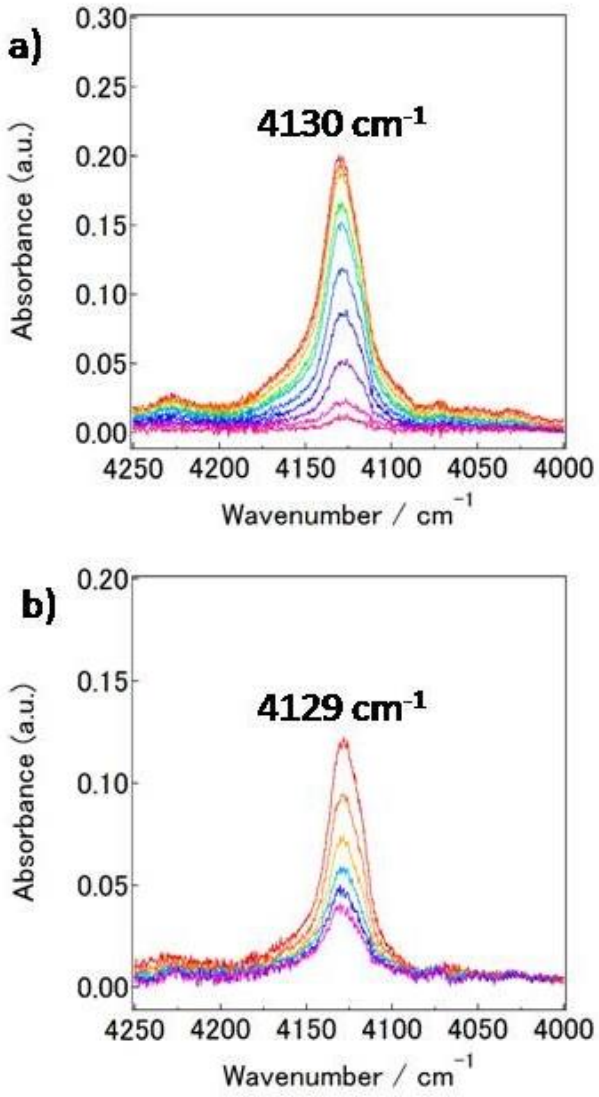

Fig. S17 Pressure- (a) and temperature- (b) dependent infrared spectra for H_2 binding within PCP-33. The resolution of in-situ IR is 0.125cm^{-1}. Background was subtracted for each spectrum.

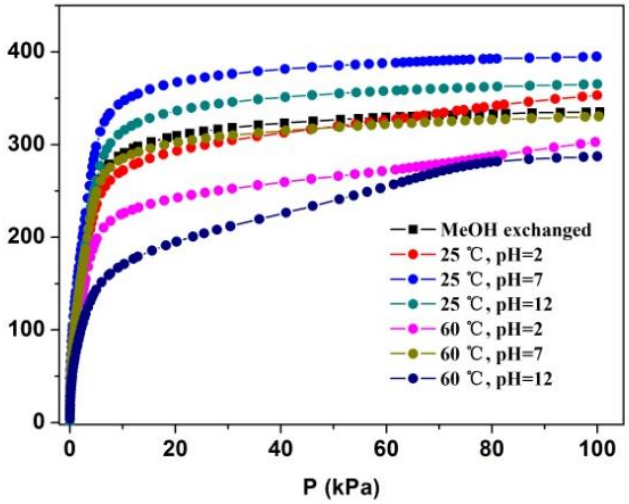

Fig. S18 CO_2 gas sorption (195 K) of water and chemical treated PCP-33.

Table S1. Langmuir-Freundlich parameters for pure component isotherms in PCP-33.

	q_{sat} mol kg^{-1}	b_0 Pa$^{-\nu}$	E kJ mol^{-1}	ν dimensionless
C_2H_2	12	1.12×10^{-8}	22	0.8
C_2H_4	12.5	6.22×10^{-8}	17.8	0.75
C_2H_6	9.5	1.85×10^{-8}	19.3	0.87
CH_4	3.7	7.19×10^{-12}	30.6	1
CO_2	9.6	2.18×10^{-10}	25.3	0.96

Table S2, Kinetic diameter of C_2H_2, C_2H_6, C_2H_4, CO_2 and CH_4

	Kinetic diameter c/Å
C_2H_2	3.3
C_2H_6	4.4
C_2H_4	4.2
CO_2	3.3
CH_4	3.8

References

Reference

(1) Sheldrick, G. M. *Acta Crystallogr. Sect. A* **2008**, *64*, 112-122.

(2) Vandersluis, P.; Spek, A. L. *Acta Crystallogr. Sect.A* **1990**, *46*, 194-201.

(3) Spek, A. L. *J. Applied Crystallogr.* **2003**, *36*, 7-13.

(4) Wu, H.; Yao, K.; Zhu, Y.; Li, B.; Shi, Z.; Krishna, R.; Li, J. *J. Phys. Chem. C* **2012**, *116*, 16609-16618.

(5) Myers, A. L.; Prausnitz, J. M. *AIChE.* **1965**, *11*, 121-130.

(6) Krishna, R.; Long, J. R. *J. Phys. Chem. C* **2011**, *115*, 12941-12950.

(7) Krishna, R. *Microporous Mesoporous Mater.* **2014**, *185*, 30-50.

(8) Duan, J.; Higuchi, M.; Krishna, R.; Kiyonaga, T.; Tsutsumi, Y.; Sato, Y.; Kubota, Y.; Takata, M.; Kitagawa, S. *Chem. Sci.*, **2014**, *5*, 660-666.

(9) Arean, C. O.; Chavan, S.; Cabello, C. P.; Garrone, E.; Palomino, G. T. *Chemphyschem* **2010**, *11*, 3237-3242.